Report
R-18-05
January 2019

Density driven mass transfer in repositories for nuclear waste

Ivars Neretnieks

SVENSK KÄRNBRÄNSLEHANTERING AB

SWEDISH NUCLEAR FUEL
AND WASTE MANAGEMENT CO

Box 3091, SE-169 03 Solna
Phone +46 8 459 84 00
skb.se

SVENSK KÄRNBRÄNSLEHANTERING

ISSN 1402-3091
SKB R-18-05
ID 1694133
January 2019

Density driven mass transfer in repositories for nuclear waste

Ivars Neretnieks
Royal Institute of Technology, KTH

Summary

In geologic repositories for nuclear waste the waste is surrounded by buffer that in practice is not permeable to water flow. The nuclides must escape by molecular diffusion to the seeping water in the fractures of the rock. At high water seepage rates the nuclides can be carried away rapidly. The seepage rate of the water can be driven by the regional hydraulic gradient as well as by buoyancy driven flow. The latter is induced by thermal circulation of the water by the heat produced by radionuclide decay. The circulation may also be induced by salt exchange between buffer and water in the fractures. A simple analytical model is developed that describes the mass transfer rate induced by buoyancy. A comparison is made with the regional gradient driven flow model.

Sammanfattning

I geologiska förvar för kärnavfall är avfallet omgivet av en buffert. Denna är i praktiken inte permeabel för vatten. Nukliderna måste ta sig till det sipprande vattnet i bergets sprickor genom molekylär diffusion. Vid högt vattenflöde i berget kan nukliderna transporteras bort snabbt. Vattenflödet kan drivas av den regionala hydrauliska gradienten såväl som av densitetsgradienter. De senare kan orsakas av uppvärmning av vattnet från värmen som produceras genom radionuklidsönderfall. Flödet kan också induceras av saltutbyte mellan buffert och vatten i sprickorna. En enkel analytisk modell har utvecklats som beskriver massöverföringshastigheten inducerad av densitetsskillnader. En jämförelse görs med den regionala gradientdrivna massöverföringshastigheten.

Contents

1 Introduction and background 7

2 Aims and scope 9

3 Mass transfer from a porous buffer to a fracture 11
3.1 Terms and expressions used to describe flow and solute transport in a fracture 11
3.1.1 Regional hydraulic gradient 11
3.2 Buoyancy induced flow 12
3.2.1 Development of simple approximate expression for buoyancy driven flow 12
3.2.2 A more accurate solution of the governing equations 12

4 Densities of clay and concrete porewaters and groundwaters 15
4.1 Groundwaters 15
4.2 Clay porewaters 15
4.3 Concrete porewaters 15
4.4 Range of density difference 15

5 Transmissivity and fracture aperture 17
5.1 Transmissivity determination 17
5.2 Fracture aperture 17

6 Examples 19

7 Discussion and conclusions 21

References 23

Appendix A note on tracer tests, channelling and leaking aquifers 25

1 Introduction and background

When modelling the release rate of radionuclides from a KBS-3 type repository for spent nuclear fuel it has been convenient to express the release rate from each canister by a concept called equivalent flow rate. The mass flowrate of a solute or a nuclide "i" can then be expressed as

$$N_i = Q_{eq} (c_o^i - c_w^i) \quad (1\text{-}1)$$

$(c_o^i - c_w^i)$ is the concentration difference between that at the interface of the buffer surrounding the canister and the approaching seeping water. Q_{eq}, with a good approximation, is independent of the type of solute or nuclide but is strongly influenced by the contact area between the water and the buffer and the by water velocity. The contact area is the product of the fracture aperture and the length of the interface between the buffer and the seeping water. The water velocity is obtained by modelling the water flow through the repository using hydraulic models. In the release model a nuclide diffuses out into the seeping water and is carried away. The release is more rapid in water with larger flowrate. This is quantified in the Qeq-model (Neretnieks et al. 2010).

The present report explores how Q_{eq} is influenced by the interaction of salt in the buffer pore water with the salt in the surrounding groundwater. The salt content influences the density of the water. If the water in the buffer has higher salt concentration than that in the water in the fracture, salt diffuses out and increases the water density in the fracture at the interface. If the concentration difference is in the other direction the density in fracture water decreases. In both cases, in sloping fractures buoyancy of the denser or lighter water will mobilise the water. The larger the density difference is, the larger is the induced velocity and the more solute will be carried to or from the buffer. For large vault repositories this phenomenon is expected to be more pronounced, the taller the repository is.

2 Aims and scope

The main aim of this contribution is to develop a simple analytic model that describes the mass transfer between a buffer and water in a fracture that is mobilised by buoyancy. The model is to be simple enough to use in stochastic simulations of radionuclide release from a repository for radioactive waste in a geologic repository in fractured crystalline rock.

3 Mass transfer from a porous buffer to a fracture

3.1 Terms and expressions used to describe flow and solute transport in a fracture

Figure 3-1 illustrates a fracture in rock in contact with a buffer surrounding nuclear waste. The fracture is modelled as a slot with smooth parallel walls with aperture δ_m. Its contact length with the material is z_o. The water flow is in the z-direction and the solute diffuses in the x-direction perpendicular to the flow-direction. After passing the slot, a solute concentration gradient has developed as illustrated by the dashed curve. The mass flowrate, N, of solute transferred to the water with initial concentration c_w can be obtained by integrating the product of flowrate and concentration from $x=0$ to infinity at $z= z_o$.

$$N= \delta_m \int_0^\infty u_z\,(x)(c(x) - c_w)dx \tag{3-1}$$

where $c(x)$ is the concentration at $z=z_o$

Two simple cases are treated. The first is when the water flow is caused by a regional hydraulic gradient. The second case is when the water flow is caused by the buoyancy generated by the in- or out-diffusion of salt that changes the density of the water.

3.1.1 Regional hydraulic gradient

In this case, as a first approximation, the flow velocity is taken to be constant everywhere in the slot. It depends not only on the regional gradient but, especially for more transmissive fractures, on the transmissivity of other surrounding fractures in the network. This may well limit the flowrate in a highly transmissive fracture.

Equation (3-1) simplifies to

$$N= \delta_m u_z \int_0^\infty (c(x) - c_w)dx \tag{3-2}$$

In analogy to heat transfer the concentration profile perpendicular to the interface along the fracture can be described by Equation (3-3) (Bird et al. 2002, p 375).

$$c(x) - c_w = (c_o - c_w)erfc(\frac{x}{2\sqrt{D_w t_w}}) \tag{3-3}$$

erfc is the complementary error function. The residence time of the water to reach z is

$$t_{w,z} = \frac{z}{u_z} \tag{3-4}$$

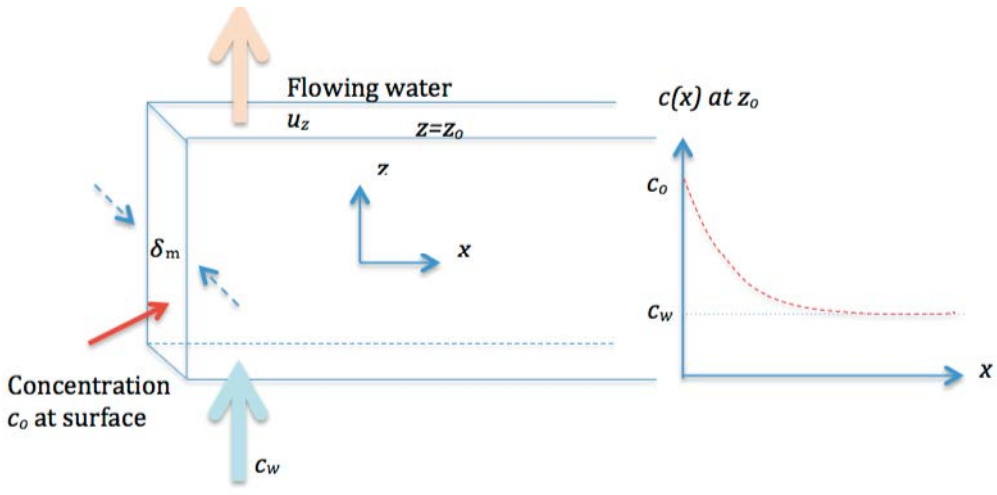

Figure 3-1. *Illustration of concentration profile in the water in a vertical slot in contact with the buffer with concentration c_o at its surface, indicated by red arrow.*

At the downstream end z_o the residence time is $t_w = \frac{z_o}{u_z}$.

At z_o integration of (3-3) gives the flowrate of solute

$$N = (c_o - c_w)\frac{2}{\sqrt{\pi}}\delta_m\, u_z\sqrt{D_w t_w} = \Delta c\frac{2}{\sqrt{\pi}}\delta_m\sqrt{D_w z_o u_z} \quad (3\text{-}5)$$

The driving force for the mass transfer is $\Delta c = (c_o - c_w)$.

The penetration depth of solute, taken to be the distance where the concentration of the solute into the water is 1 % of $(c_o - c_w)$, is obtained from (3-3)

$$\eta_{0.01} = 3.64\sqrt{D_w t_w} \quad (3\text{-}6)$$

For Equation (3-2) to be valid $\eta_{0.01} \gg \delta_m$. Otherwise, the friction at the buffer interface cannot be neglected.

In practice in fractures in the bedrock, the aperture δ_m can not be measured, but the transmissivity of the slot T can. The flow is driven by the hydraulic gradient $\frac{dh}{dz}$, where h is the hydraulic head. This can also be assessed by measurement or by hydraulic modelling. The velocity is related to these entities by

$$u_z = \frac{T}{\delta_m}\frac{dh}{dz} \quad (3\text{-}7)$$

Introducing (3-7) into (3-5) gives

$$N = \Delta c\frac{2}{\sqrt{\pi}}\sqrt{D_w z_o T\,\delta_m\frac{dh}{dz}} \quad (3\text{-}8)$$

3.2 Buoyancy induced flow

3.2.1 Development of simple approximate expression for buoyancy driven flow

When solute concentration influences the density of the water near the buffer this sets the water in motion, up or down, depending on if the water at the surface becomes less or more dense. Then the integral in Equation (3-1), $\int_0^\infty u_z(x)(c_o(x) - c_w)dx$, must account for simultaneous variations in velocity and concentration. They influence each other and that mutual effect must be derived.

We first derive an approximate solution that conceptually is very simple and that later is shown to be surprisingly accurate compared to the exact solution. The approximate solution is obtained by neglecting the influence on the concentration profile by the velocity profile. Assuming that the concentration profile in the density-driven case can be *approximated* by the same expression as for the constant velocity case and that the relation between water density and solute concentration is linear, $\Delta\rho = \alpha(c_o - c_w)$, a vertical hydraulic gradient $\frac{\Delta\rho(x=0)}{\rho} = \frac{dh}{dz}$ will result at the boundary between the water and the buffer. Equation (3-8) then may be used as an approximation. The error caused by describing the concentration profile by Equation (3-3) is assessed in the next section by comparison with a more accurate solution.

It should be noted that density-driven flow can be induced also in sloping fractures, isolated from or connected to a network that does not allow much of the regional gradient to generate flow through it. Then internal circulation in the fracture still can develop and generate mass transfer to or from a deposition hole or a vault repository.

In the next section, a so tall fracture is modelled that it can be approximated to be infinite and that circulation does not have to be considered. It suffices to consider only the region nearest to the buffer/water interface. This approximation can be used when the solute penetration depth $\eta_{0.01} \ll z_o$, the length (height) of the interface and of the horizontal extent of the fracture.

3.2.2 A more accurate solution of the governing equations

The equations that govern the flow and salt transport in a vertical narrow two-dimensional slot are summarized below. p is pressure, μ water viscosity, ρ is density and g the gravitation constant.

$$\frac{\partial u_x}{\partial x} + \frac{\partial u_z}{\partial z} = 0 \quad (3\text{-}9)$$

$$u_x = -\frac{k}{\mu}\frac{\partial p}{\partial x} \quad (3\text{-}10)$$

$$u_z = -\frac{k}{\mu}\left(\frac{\partial p}{\partial z} + \rho g\right) \quad (3\text{-}11)$$

$$\frac{\partial c}{\partial t} = -u_x\frac{\partial c}{\partial x} - u_z\frac{\partial c}{\partial z} + D_w\left(\frac{\partial^2 c}{\partial x^2} + \frac{\partial^2 c}{\partial z^2}\right) \quad (3\text{-}12)$$

$$\rho = \rho_o(1 + \alpha c) \quad (3\text{-}13)$$

The considered region extends from x=0 to ∞ and from $z = -\infty$ to ∞. On the boundary at $x = 0$ the concentration $c = c_o$ for $z > 0$ and the far-away water has concentration c_w.

For the problem at hand when only buoyancy generated flow acts it is assumed that the velocity and concentration profiles have attained a steady state. This can be attained for times much longer than the water to reach z_o. Then $\frac{\partial c}{\partial t}$ can be neglected and the problem becomes time independent. An analytical solution to this problem has been derived by Ene and Poliševski (1987, Chapter 4). From their results, Equation (3-8) can be derived. It gives 1.3 times smaller values for the constant $\frac{2}{\sqrt{\pi}}$. The driving force $\frac{dh}{dz}$ is then given by that induced by buoyancy due to the density difference $\frac{\Delta\rho(x=0)}{\rho}$. Also, the penetration depth $\eta_{0.01}$ is somewhat different with a constant 6.31 instead of 3.64 in Equation (3-6). The shape of the concentration profile is also different.

It was surprizing that the very simple approximate solution method resulted in the exact solution of the set of Equations 3-9 to 3-13 except for a constant factor difference of 1.3.

The same equations apply for flow through a porous medium in contact with the buffer. Then $\delta_m = \delta_{zone}$ where δ_{zone} is the thickness of the zone and ε its porosity.

An illustrative way of describing the release and transport capacity of the water flowing past e.g. a deposition hole for a canister with nuclear waste such as in the KBS-type repository is the concept of the equivalent flowrate mentioned earlier. It is the solute release rate N divided by the driving force (Neretnieks et al. 2010). $Q_{eq} = N/\Delta c$. It has been useful when integrating radionuclide release and transport modelling with models that simulate water flow through and past repositories with a multitude of sources.

To apply these results, information on repository conditions is needed on density differences $\Delta\rho$, transmissivities T and apertures δ_m of the real fractures. This is treated in the next two sections.

4 Densities of clay and concrete porewaters and groundwaters

Two materials that are used to enclose the radioactive waste are bentonite clays and concrete. Both materials are porous and the porewaters contain salts that can diffuse out or into the groundwater depending on where the concentration is largest. Only an outline of potential concentrations is presented in order to quantify the expected range of density differences. This will later be used in an illustrative example. As first approximation, the density difference can be set to $\Delta\rho \cong \Delta c$ when c has unit kg/m^3, Equation (3-13).

4.1 Groundwaters

The salt content of groundwaters varies with location, depth and time. At Forsmark, the site selected for the Swedish repository for spent fuel (SKB 2008) the intermediate depth groundwaters (200–600 m) at present have salinity between 2 and 10 kg/m^3. Deep groundwaters (>600 m) can have more than 10 and shallow water have mostly less than 2 kg/m^3. At larger depths, the salinity can be much higher than that in the oceans 35 kg/m^3.

4.2 Clay porewaters

Bentonite porewaters will be influenced by the dissolution of the minerals in the bentonite (Savage et al. 2011) in their simulations predict ionic strengths ranging from 0.09 to 0.384 mol/l. The components include calcium, sodium, magnesium, sulphate, carbonate and other ions. Specific compositions are not presented. Assuming a mean molar mass of 60 g/mol gives concentrations between 5.4 and 23 kg/m^3.

4.3 Concrete porewaters

Andersson et al. (1989) pressed porewater from 7 different concretes, mostly based on Portland cement, with different additives. Na and K were the dominating cations with concentrations from 0.3–3.2 kg/m^3 Na and 0.1–7.5 kg/m^3 K. pH varied between 12.4 to 13.5. Total salt concentrations were between 1.7 and 11.8 kg/m^3.

4.4 Range of density difference

The density differences between the pore- and groundwaters can be expected not to exceed a few tens of kg/m^3 and the density-induced gradient, $\frac{\Delta\rho(x=0)}{\rho}$, would not exceed a few percent at repository depth even when meteoric water invades over long times. This is an order of magnitude, or more, larger than typical hydraulic gradients at repository depth (SKB 2008).

5 Transmissivity and fracture aperture

5.1 Transmissivity determination

The transmissivity of fractures in rock in-situ can be measured by several techniques in boreholes. See e.g. Ripatti et al. (2013). The principle is to induce a hydraulic head difference between the borehole and the far away water in the fractured rock. From the measured flowrate to or from each location with an identified fracture and the head difference, the transmissivity T of the fractures can be determined.

5.2 Fracture aperture

Fracture apertures cannot be measured in-situ. From transmissivity data, estimates of the aperture can be made by the cubic law. This is valid for laminar flow in a parallel aperture slot with smooth walls but is not necessarily a proper measure of the *mass balance aperture* δ_m. This is the aperture that describes the volume of water per fracture area and could also account for the presence of infill and for fracture zones.

The *cubic law aperture* describes the relation between transmissivity and aperture for an ideal slot with smooth walls when flow is laminar.

$$\delta_c = (12\, T \frac{\mu_w}{\rho_w g})^{1/3} \qquad (5\text{-}1)$$

δ_c is "cubic law" aperture, T is fracture transmissivity, μ_w and ρ_w are viscosity and density of water and g is the gravitation constant. δ_c is well correlated to the mechanical aperture in real fractures (Witherspoon et al. 1980). δ_c is expected to give a fair approximation of the mass balance aperture δ_m for smooth walled variable aperture fractures. In fractures with rough walls the mass balance aperture can differ from what might be perceived as a mechanical aperture. Tsang (1992) showed that the mass balance aperture always must be larger or equal to the cubic law aperture. For fracture zones where the main resistance to flow is caused by the presence of particles filling in the fracture this is better modelled as a slot filled with a porous medium with a given thickness and porosity. The mass balance aperture then is the zone thickness times its porosity.

Attempts have been made to use in-situ tracer experiments to determine δ_m. Experimentally the mass balance aperture can be estimated from the fracture volume and the resince time t_w for a flowrate Q through this volume. One often-used technique to do this is by in-situ tracer tests. By pumping water out from a section in a borehole that intersects a fracture and measuring the residence time of the water by a tracer injected into the same fracture at a certain distance from the pumping hole, the aperture can be derived. Assuming that the fracture has reasonably similar properties everywhere, the volume of the water is taken to be the aperture times the area of a circle with the radius equal to the distance between injection and pumping hole. This determines the residence time of the flowrate Q. As the distance between the boreholes, r is very much larger that the radii of the boreholes the mass balance aperture is obtained from

$$\delta_m = \frac{Q t_w}{\pi r^2} \qquad (5\text{-}2)$$

For this technique to be valid it is *essential* that all flowrate to the pumping location passes the intended fracture and that the measured residence time is representative of the entire fracture. If there is mal-distribution of flow by so-called channelling and the tracer is injected the fast channel, which makes up a fraction β of the entire fracture, δ_m can be over-estimated by a fraction $1/\beta$. Considering that the pumping location will probably be chosen in a fracture where a high transmissivity location is intersected β is probably small. If the injection is made in a slow channel the residence time could be dominated by the time to for this flow to reach either the pumping hole or to intersect the fast channel somewhere. This aggravates the problem considerably. Also if the fracture has been fed by water from intersecting fractures in a leaking rock matrix, Q in (5-2), is overestimated and the aperture would also be over-estimated. This is discussed in more detail in the appendix.

(Hjerne at al. 2010) analysed 74 in-situ experiments from 6 different sites. They found that δ_m was about 100 times larger than δ_c over a range of fracture transmissivities from 10^{-9} to 10^{-3} m^2/s. For the transmissivity 10^{-9} m^2/s, a very tight fracture, their δ_m aperture is 0.4 mm. For a transmissivity of 10^{-6} m^2/s, it is 4 mm. It may be noted that 4 mm aperture open single fractures have not been observed in tunnels and drifts in crystalline rocks.

Similar discrepancies between δ_m and δ_c were found in the so-called TRUE experiments (Neretnieks and Moreno 2003). At this site, transmissivities had been measured in boreholes surrounding the pumping and tracer injection boreholes. These showed that the target fracture, called feature A, must be intersected by many water-conducting fractures, from which inflow contributed considerably to the pumping flowrate. Such information on fracture networks surrounding the target fracture is not available for the Hjerne et al. (2010) evaluations.

6 Examples

In the following two examples we illustrate that diffusion of salt from the buffer or backfill around a repository for nuclear waste to the seeping water in the rock fractures, (or vice versa) by generating buoyancy driven flow can *induce* considerable mass transfer of radionuclides to the seeping water. We do the comparison by comparing the *induced mass* transfer rate expressed as the equivalent flowrate $Q_{eq,}$ with that induced by the "natural" hydraulic gradient in the rock. The concept of the equivalent flowrate is used by SKB to calculate mass transfer of solutes to or from canisters and vaults in a repository for nuclear waste in performance assessment calculations.

Consider a vault with two vertical sides 20 m high that is intersected by a vertical fracture. Figure 6-1 shows $Q_{eq} = 2N/\Delta c$ based on Equation (3-8) as function of fracture transmissivity for two different gradients and when using cubic law aperture δ_c for δ_m. The "2" in the expression for Q_{eq} means that the mass transfer to both sides of the vault intersected by the fracture are accounted for. The expressions used for N in the example are

$N = \Delta c \frac{2}{\sqrt{\pi}} \sqrt{D_w z_o T \, \delta_c \frac{dh}{dz}}$ where $\delta_c = (12\, T \frac{\mu_w}{\rho_w g})^{1/3}$ and $\frac{dh}{dz}$ is the hydraulic gradient in the rock mass surrounding the vault.

For gravity-driven flow the gradient is caused by the density difference between the far-away water and the water at the interface of the vault, $\frac{\Delta\rho(x=0)}{\rho}$ and Q_{eq} will be 1.3 times lower as explained in section 3.2.2.

This figure captures the main results and influences. It gives Q_{eq} as function of the transmissivity of the fracture with gradient as parameter. The gradient for the gravity-driven flow depends only on the concentration/density difference between the pore water in the buffer and the far away water in the fracture. It is seen from Equation (3-8) that scaling to another mass balance aperture can be done simply. The solution depends on the following way on the central entities: $\sqrt{D_w z_o T \, \delta_m \frac{dh}{dz}}$. A larger or smaller vertical extent z_o, as well as the mass balance aperture, scale by the square root of the magnitude of these entities. Should one e.g. believe that the mass balance aperture δ_m is 100 times larger than δ_c, as indicated by Hjerne et al. (2010) then the results change by a factor 10.

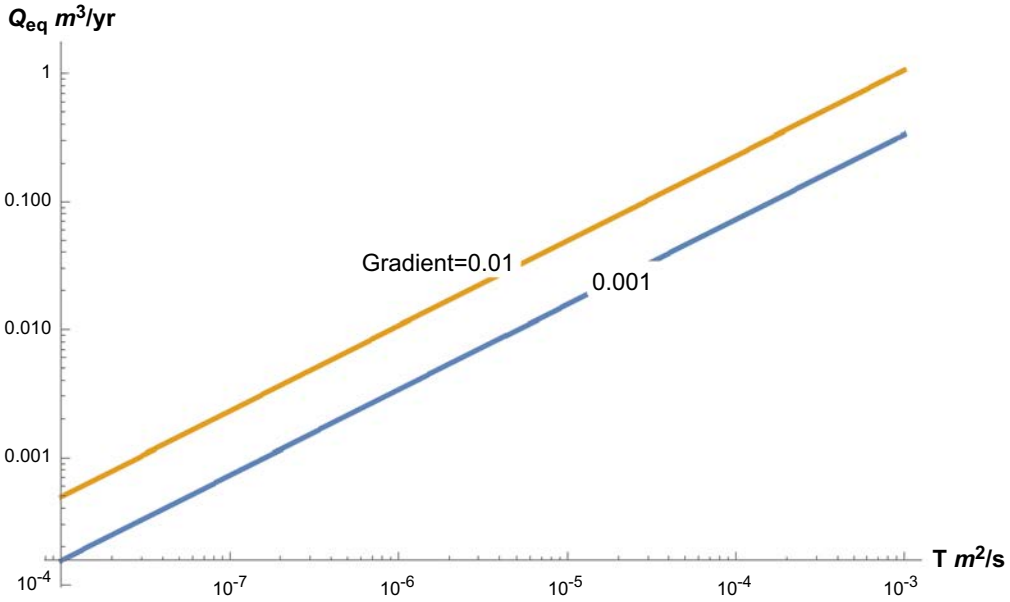

Figure 6-1. *Q_{eq} as function of fracture transmissivity for two different hydraulic gradients.*

In another illustration, consider a vault, 20 m high and 20 m wide with 1 m thick bentonite buffer between the walls and the waste. The vault is intersected by a fracture and water can flow on both vertical sides generating a Q_{eq} of 0.01 m^3/yr. The porosity of the bentonite is 50 %. On each side of the fracture along the vault a 1 m long bentonite section is accessible by diffusion to the fracture intersection. The water in the pore volume of the bentonite that can exchange solute with the flowing water on both sides of the vault is $(20^2-18^2)\times 2\times 0.5 = 76$ m^3. This gives a fraction $\frac{Q_{eq}}{V_w} = 1.3\times 10^{-4}$ yr^{-1} of the solute concentration difference that will be exchanged per year. The buoyancy induced flow can last for a long time under these conditions.

7 Discussion and conclusions

The buoyance can also be caused by temperature differences generated by heat producing nuclear waste such as spent nuclear fuel which can heat the buffer material by several tens of degrees °C, over long times. The same equations can be used.

The buoyance driven mass transfer and that induced by a hydraulic gradient are very similar. The former results in 30 % smaller transfer rates when compared for the driving forces caused by the regional hydraulic gradient and the local density difference $\frac{dh}{dz}$ and $\frac{\Delta\rho(x=0)}{\rho}$ respectively. The buoyancy induced gradient can be expected to be on the order of a few % and less. The buoyancy driven flow will decrease with time as the concentration difference between the buffer and the flowing decreases over time.

The decrease rate can be illustrated in the following way. Assume that the pore water in a part of the buffer in the vault straddling the fracture is always well mixed. If the water volume in the buffer that can be equilibrated is V_w and the equivalent flowrate is Q_{eq}, the concentration difference Δc between buffer water and flowing water changes in time as

$$\Delta c(t) = \Delta c(t=0) \times Exp(-\frac{Q_{eq}}{V_w} t) \qquad (7\text{-}1)$$

There is a large difference between the cubic law derived data and those presented by Hjerne et al. (2010), about a factor of 100. At present, it seems likely that the actual mass balance aperture is closer to the cubic law aperture for individual fractures. The tracer derived aperture data may not be meaningful for either individual fractures or for fracture zones.

More discussion of and information on fracture apertures is presented in the appendix where it is concluded that mass balance apertures obtained from pumping tests based on observed tracer residence times are likely to overestimate mass balance apertures orders of magnitude.

The findings above can be used in the following way. First, one has to assess the potential difference between the concentration of salts in the groundwater and the pore water in the buffer in the repository and the density difference this can cause, $\frac{\Delta\rho(x=0)}{\rho}$. If this is less than the hydraulic gradient in the rock mass, impact of the buoyancy induced flow and thus the equivalent flowrate Q_{eq} can be neglected. If the opposite is found, it cannot be neglected and must be accounted for in the modelling of mass transfer between repository and the flowing water in the rock mass.

References

SKB's (Svensk Kärnbränslehantering AB) publications can be found at www.skb.com/publications.

Abelin H, Gidlund J, Moreno L, Neretnieks I, 1983. Migration in a single fissure in granitic rock. In McVay G L (ed). Scientific basis for nuclear waste management VII: symposium held in Boston, Massachusetts, 14–17 November 1983. New York: North-Holland. (Materials Research Society Symposium Proceedings 26), 239–246.

Abelin H, Moreno L, Tunbrant S, Gidlund J, Neretnieks I, 1985. Flow and tracer movements in some natural fractures in the Stripa granite. Results from the Stripa project Phase I In Proceeding of NEA Information Symposium on In Situ Experiments in Granite Associated with the Disposal of Radioactive Waste, Stockholm, 4–6 June 1985. Paris: OECD/NEA, 67–81.

Abelin H, Birgersson L, Neretnieks I, Ågren T, 1989. A channeling experiment to study flow and transport in natural fractures In Lutze W, Ewing R C (eds). Scientific basis for nuclear waste management XII: symposium held in Berlin, 10–13 October 1988. Pittsburgh, PA: Materials Research Society. (Materials Research Society Symposium Proceedings 127), 661–668.

Abelin H, Birgersson L, Ågren T, Neretnieks I, Moreno L, 1990. Results of a channeling experiment in Stripa. In Proceedings GEOVAL 90, Symposium on Validation of Geosphere Flow and Transport Models, Stockholm, 14–17 May 1990. Paris: OECD/NEA, 157–164.

Abelin H, Birgersson L, Gidlund J, Neretnieks I, 1991a. A large scale flow and tracer experiment in granite: I. Experimental design and flow distribution. Water Resources Research, 3107–3117.

Abelin H, Birgersson L, Moreno L, Widén H, Ågren T, Neretnieks I, 1991b. A large scale flow and tracer experiment in granite II. Results and interpretation. Water Resources Research 27, 3119–3135.

Abelin H, Birgersson L, Widén H, Ågren T, Moreno L, Neretnieks I, 1994. Channeling experiments in crystalline fractured rocks. Journal of Contaminant Hydrology 15, 129–158.

Andersson K, Allard B, Bengtsson M, Magnuson B, 1989. Chemical composition of cement porewaters. Cement and Concrete Research 19, 327–332.

Bird R B, Stewart W E , Lightfoot E N, 2002. Transport phenomena. 2nd ed. New York: Wiley.

Birgersson L, Neretnieks I, 1988. Diffusion in the matrix of granitic rock. Field test in the Stripa mine. Final report. SKB TR 88-08, Svensk Kärnbränslehantering AB.

Byegård J, Hakami E, Hjerne C, Nordqvist R, Cvetkovic V, Drake H, Tullborg E-L, Winberg A, 2017. TRUE-1 Completion. Final report. SKB TR-12-11, Svensk Kärnbränslehantering AB.

Ene H I , Poliševski D, 1987. Thermal flow in porous media. Dordrecht: Reidel.

Hjerne C, Nordqvist R, Harrström J, 2010. Compilation and analyses of results from cross-hole tracer tests with conservative tracers. SKB R-09-28, Svensk Kärnbränslehantering AB.

Moreno L, Svensson E, Neretnieks I, 2001. Determination of the flow-wetted surface in fractured media. In Hart K P, Lumpkin G R (eds). Scientific basis for nuclear waste management XXIV: symposium held in Sydney, Australia, 27–31 August 2000. Warrendale, PA: Materials Research Society. (Materials Research Society Symposium Proceedings 663), 869–874.

Neretnieks I, 1980. Diffusion in the rock matrix: an important factor in radionuclide retardation? Journal of Geophysical Research 85, 4379–4397.

Neretnieks I, 2002. A stochastic multi-channel model for solute transport- Analysis of tracer transport in fractured rock. Journal of Contaminant Hydrology 55, 175–211.

Neretnieks I, 2006. Channeling with diffusion into stagnant water and into a matrix in series. Water Resources Research 42, W11418. doi:10.1029/2005WR004448

Neretnieks I, 2017. Solute transport in channel networks with radial diffusion from channels in a porous rock matrix. SKB R-15-02, Svensk Kärnbränslehantering AB.

Neretnieks I, Moreno L, 2003. Prediction of some in situ tracer tests with sorbing tracers using independent data. Journal of Contaminant Hydrology 61, 351–360.

Neretnieks I, Abelin H, Birgersson L, 1987. Some recent observations of channeling in fractured rocks – its potential impact on radionuclide migration. In Buxton B E (ed). Proceedings of the Conference on Geostatistical, Sensitivity and Uncertainty Methods for Ground-Water Flow and Radionuclide Transport Modeling, San Francisco, 15–17 September 1987. Columbus: Battelle, 387–410.

Neretnieks I, Liu L, Moreno L, 2010. Mass transfer between waste canister and water seeping in rock fractures. Revisiting the Q-equivalent mode. SKB TR-10-42, Svensk Kärnbränslehantering AB.

Neretnieks I, Moreno L, Liu L, Mahmoudzadeh B, Shahkarami P, Maskenskaya O, Kinnbom P, 2018. Use of infrared pictures to assess flowing channel frequencies and flowrates in fractured rocks. A feasibility study. SKB R-17-04, Svensk Kärnbränslehantering AB.

Ripatti K, Komulainen J, Pöllänen J, 2013. Difference flow and electrical conductivity measurements at the Olkiluoto site in Eurajoki, drillholes OL-KR56, OL-KR57 and OL-KR57B. Posiva Working Report 2013-26, Posiva Oy, Finland.

SKB, 2008. Site description of Forsmark at completion of the site investigation phase. SDM-Site Forsmark. SKB TR-08-05, Svensk Kärnbränslehantering AB.

Savage D, Arthur R, Watson C, Wilson J, Strömberg B, 2011. Testing geochemical models of bentonite pore water evolution against laboratory experimental data. Physics and Chemistry of the Earth 36, 1817–1829.

Tsang C-F, Neretnieks I, 1998. Flow channeling in heterogeneous fractured rocks. Reviews of Geophysics 26, 275–298.

Tsang Y W, 1992. Usage of "equivalent apertures" for rock fractures as derived from hydraulic and tracer tests. Water Resources Research 28, 1451–1455.

Winberg A, Andersson P, Hermanson J, Byegård J, Cvetkovic V, Birgersson L, 2000. Äspö Hard Rock Laboratory. Final report of the first stage of the tracer retention understanding experiments. SKB TR-00-07, Svensk Kärnbränslehantering AB.

Witherspoon P A , Wang J S Y, Iwai K, Gale J E , 1980. Validity of Cubic Law for fluid flow in deformable rock fracture. Water Resources Research 16, 1016–1024.

Wolfram, 2018. Wolfram Mathematica 11. Available at: https://www.wolfram.com/mathematica/

Appendix

A note on tracer tests, channelling and leaking aquifers

A1 Summary

Fracture apertures cannot be determined in-situ in fractured crystalline rocks with presently available techniques. Tracer tests have been used in attempts to do so but there are indications that such tests can grossly overestimate the size of the aperture that contains the mobile water. The impacts of some assumptions underlying the interpretations are discussed. One is that fractures can be conceived and quantitatively modelled as evenly open over their entire size. The other is that the rock matrix in contact with the fracture is essentially tight and thus does not leak any water near the section where the between-hole tracer test is made. It is shown that the first assumption is unrealistic because by far most of the water flows only in a small fraction of the fracture, so-called channelling. The assumption that the fracture is not subject to leakage from the rock matrix was also found to be very shaky in the evaluation of a well-documented field experiment at Äspö HRL where the rock mass surrounding the target fracture had been extensively investigated.

Channelling and leaking are likely to cause orders of magnitude exaggeration of the magnitude of the mass balance apertures.

A2 Introduction and background

The Swedish and Finnish repositories for radioactive waste are and will be located in fractured crystalline rock, high-level and long-lived wastes at around 500 m depth and low- and intermediate-level wastes are placed at a shallower depth. Water flows in fractures and fracture zones and will carry leaking nuclides to the biosphere. The transmissivities, mobile water volumes and fracture apertures in the complex fractures and channel networks influence the carrying capacity of the water, its residence time distribution and the transfer rate from the repository to the mobile water. This short note revisits the methods to assess fracture apertures and points out some pitfalls.

The magnitude of the physical aperture can influence the performance of a repository in fractured rocks in several ways. One reason is that seeping water in fractures in contact with a buffer or backfill surrounding the packages with the waste will be contaminated with nuclides roughly in proportion to the size of the aperture of a fracture in contact with the water because of the larger area for mass transfer. Another reason is that a larger aperture fracture will allow more bentonite buffer material to be lost. Buffer loss can be especially sensitive to the physical aperture of the fracture because the expanding bentonite behaves as a non-Newtonian fluid, which can intrude much easier in larger fractures than in small fractures. It is not possible with present-day methods to reliably determine fracture apertures in-situ although some information can be derived from borehole and bore-core observations. One of the problems is that boreholes only sample a very small part of a fracture and may not find the more open location in variable aperture fractures in which water flows in preferential locations- channels. Tracer tests are supposed to give information on the flowpaths that actually are used by the seeping water and are used to assess the aperture available to flow.

The main aim of this note is to explore the assumptions commonly used for interpreting tracer tests and to try to quantify errors that may arise when the assumptions are not upheld. It is shown that numerous tracer tests evaluations predict order to orders of magnitude larger apertures than the commonly used cubic law method based on hydraulic transmissivity and what can be supported by physical observations in the field.

A3 Tracer tests in fractured rocks

One of the aims of tracer tests in fractured rocks is to obtain information on the fracture apertures. Tsang (1992) discusses different ways to define fracture apertures and their physical meaning. The fractures are often modelled as circular disks or other thin flat objects. Two or more boreholes are drilled into the rock and a fracture is selected with higher transmissivity than other neighbouring fractures. In each of the boreholes that intersect the selected fracture one or more borehole sections are isolated by packers. In a section in one borehole water is pumped out with a constant flowrate. In the other hole(s) a small water volume with tracer is added. This water flows to the pumping

location. The arrival of the tracer is monitored in the pumping section and the mean residence time t_w of the tracer is determined from the concentration breakthrough curve. The mean fracture aperture δ_m can then be obtained from

$$\delta_m = \frac{Qt_w}{\pi r^2} \qquad \text{(A-1)}$$

where Q (m^3/s) is the pumping rate and r (m) the distance between the two boreholes. The borehole diameters are negligible compared to r. δ_m is called *mass balance aperture.*

One central assumption in using (A-1) when evaluating the tracer tests in fractures in-situ is that the fracture walls are impermeable and that there is no leakage of water from the rock matrix that would increase Q above the flowrate that entered the fracture at a distance larger than the injection location. Another assumption is that the transmissivity and thus the velocity is reasonably homogeneous over the entire fracture area. In variable aperture fractures t_w(s) can be considerably influenced by the local aperture near the injection point. Natural, variable aperture fractures are known to have widely different transmissivities and to develop channelling (Tsang and Neretnieks 1998). Seldom more than a few injection boreholes have been used to test the same fracture. If only a fraction of the pumped flow has passed the selected fracture the entire distance r, and the rest has arrived from other fractures that intersect the selected fracture somewhere between pumping and injection hole, the pumping flowrate is not representative for the intended test. Similarly, if the tiny volume of the traced water was injected in a location with low transmissivity, the measured residence time may be much larger than the mean. The residence time in the early part of the flowpath in a radially converging tracer test is especially sensitive to local transmissivity variations. A lower local velocity in the first fraction of the flow flowpath from the injection location will considerably add to the residence time along that path.

A3 Transmissivity and fracture aperture

In an ideal slot and for laminar flow the relation between aperture and transmissivity is obtained from Equation (A-2). Witherspoon et al. (1980) showed in a series of experiments where fractures were subject to stress up to 20 MPa and where the change of aperture was monitored, that the cubic law was valid for fracture apertures ranging from 3 to several 100 μm under laminar flow. The deviation from the cubic law was at most a factor 1.5, but mostly much less. For smooth, parallel walled fractures, the mechanical aperture is also a measure of the volume of the fracture with a given area that can be filled with mobile water. This is called the *mass balance aperture*.

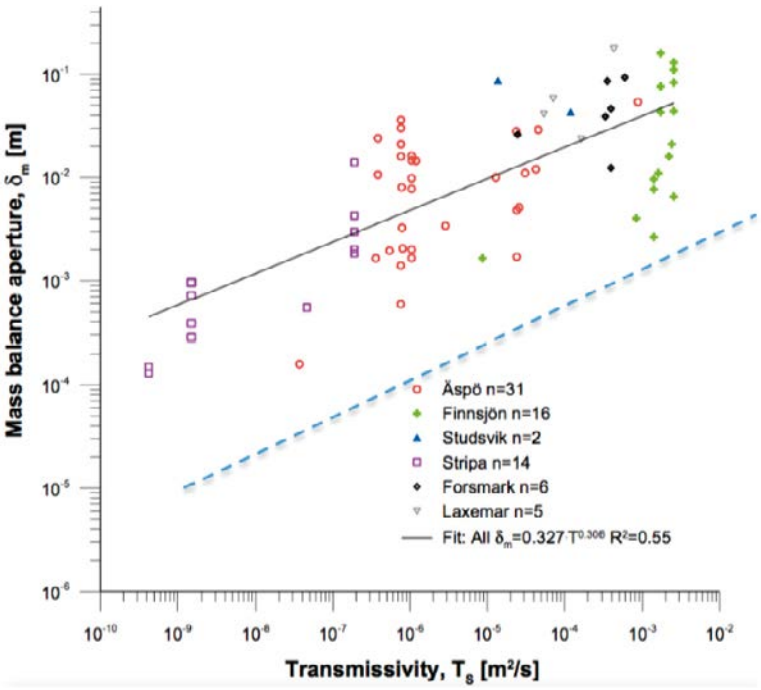

Figure A-1. *Mass balance δ_m aperture (Hjerne et al. 2010) and cubic law δ_c, dashed line.*

The cubic law aperture is derived from hydraulic measurements assuming laminar flow between two parallel walls.

$$\delta_c = (12\, T \frac{\mu_w}{\rho_w g})^{1/3} \quad \text{(A-2)}$$

Hjerne et al. (2010) compiled data on transmissivities and evaluated mass balance apertures, δ_m, from 6 different sites, in total 72 tests. 40 of these were in fractures characterized as fracture zones and 32 as single fractures. All transmissivities above 10^{-6} m^2/s are for the zones.

δ_m was found to be nearly 100 times larger than δ_c. A fit to these data gives

$$\delta_m = 0.327\, T^{0.306} \quad \text{(A-3)}$$

These data show that on the average δ_m is about 100 times larger than δ_c.

A4 Some potential causes for overestimation of fracture apertures

A4.1 Matrix diffusion

The rock matrix has microscopic connected pores into which tracers can diffuse, This gives a tracer access to more water than that seeping in the fracture. The tracer residence time will be larger than the flowing residence time. The larger the flow wetted surface, FWS, per flowrate Q is, the larger will be the retardation of the tracer and the larger the fracture aperture will seem to be. In fractures with low transmissivity and under low gradients the effect can be enormous (Neretnieks 1980). For the high flowrates in forced tracer tests, the effect is usually not very important unless the fracture contains fault-gouge and small broken rock fragments. Then the large surface area of the fragments and especially the small particles can add to accessible water volume.

A4.2 Channeling

Natural fractures have variable aperture, which leads to channelling (Tsang and Neretnieks 1998). Water that flows in a fracture seeks out preferential pathways and most of the water flows in a small fraction of the entire fracture volume. The residence time measured in a converging pumping test will be much influenced by where and how the tracer is injected. If a very small volume is injected in a location with low transmissivity it can take a long time for it to reach the stream with a more rapid flow that carries most of the water to the pumping hole. Very seldom more than one or a few injection locations in the selected fracture have been used and it is difficult to estimate the error that this effect can induce.

Numerous experiments and observations in the field have shown that water seeps out from rock faces in “channels” with widths varying from less than a cm up to tens of cm (Abelin et al. 1983, 1985, 1989, 1990, 1991 a, b, 1994, Birgersson and Neretnieks 1988, Neretnieks et al. 1987, 2018, Tsang and Neretnieks 1998). In none of these investigations have visually observed apertures approaching 1 mm been seen. Usually, channels are cm to tens of cm wide. The distances between channels in the fracture plane are usually much larger than the channel width. This implies that the mean fracture aperture must be much smaller than 1 mm. Visually observed and measured apertures are approximately equal to mechanical apertures. At least locally, the mechanical aperture would also be a reasonable first approximation of the mass balance aperture in individual fractures.

Adjacent to the more rapidly flowing portions of the channels there are slower portions and in practice stagnant water. This water can be accessed by diffusion and have the same retarding effect as matrix diffusion. It has been found to be able to cause considerable retardation in field tracer experiments (Abelin et al. 1991 a, b). Neretnieks (2002) suggested that this might be one of the causes for the unreasonably large fracture apertures found using Equation (1) to evaluate the TRUE experiment (described in chapter 6 below). Neretnieks (2006) showed that the diffusion into stagnant waters, which gives access to additional area for matrix diffusion can contribute to the tracer retardation. Furthermore, in channels, the matrix diffusion becomes more radial after some time, which speeds up the access to matrix porewaters (Neretnieks 2017).

A4.3 Leaking fractures

Fractures intersect other fractures. Fractures vary enormously in size and large fractures can be intersected by a multitude of smaller fractures. The connected channels in these fractures form complex 3-dimensional networks. A fracture used in a tracer experiment can be intersected by fractures between the pumping location and the tracer injection location and fed by water from these intersecting fractures. This is called a leaking fracture in analogy to "leaking aquifer". Although often, hydraulic tests are made between the selected pumping and injection location and other locations in boreholes in the vicinity such tests cannot give detailed information of the transmissivity distribution and the potential magnitude of leakage. From our own experience and especially from the five experiments, in the Stripa underground research laboratory, it is not possible with present day tools to assess any details of the geometric and hydraulic properties of the channel networks inside the rock.

This short appendix focuses mainly on the potential impact of leaking fractures to explore if this can at least partly explain the surprisingly large fracture apertures reported based on pumping tracer tests.

A5 Modelling tracer test in a leaking fracture

Consider a case where the rock surrounding the fracture is not tight and can be described as a homogeneous porous medium with a conductivity K and an undisturbed hydraulic head h_∞ (m) at some distance z_o (m) from the fracture. When the head in the packed off section in the pumping hole has been dropped and stabilized at h_i, steady state is established. The circular fracture has radius r_o. The fracture size is much larger than the distance between the pumping and injection hole(s).

Figure A-2 Illustrates a fracture for a tracer test in fractured rock with a network of conducting fractures. The region is z_o high, including the selected fracture and has radius r_o. At the top and right boundaries, the hydraulic head is maintained at h_∞. The lower and left are closed or symmetry boundaries. The fracture network above the selected fracture has a mean hydraulic conductivity K (m/s).

At steady state the hydraulic head in the fracture and the surrounding rock is described by a cylindrical region with $r_i < r < r_o$ and with $0 < z < z_o$

$$K(z)\frac{1}{r}\frac{\partial}{\partial r}\left(r\frac{\partial h}{\partial r}\right)+\frac{\partial}{\partial z}\left(K(z)\frac{\partial h}{\partial z}\right)=0 \qquad \text{(A-4)}$$

$K(z)$ is the hydraulic conductivity of the rock, including the fracture. For the fracture $K = T/\delta$, where T is the transmissivity of the fracture, which can be measured and δ is its aperture, which cannot be measured but a lower bound can be estimated by the cubic law. The term $\frac{\partial}{\partial z}\left(K(z)\frac{\partial h}{\partial z}\right)$ is simplified to $K(z)\frac{\partial^2 h}{\partial z^2}$ for the numeric solution because $K(z)$ is expressed by a Heaviside step function with one value for the fracture $K_{frac} = T/z_i$ and another constant value for the rock, K_{rock}. For numerical convenience, the fracture is modelled as a thin porous medium with a thickness z_i, larger than the aperture, but much smaller than the vertical extent of the medium.

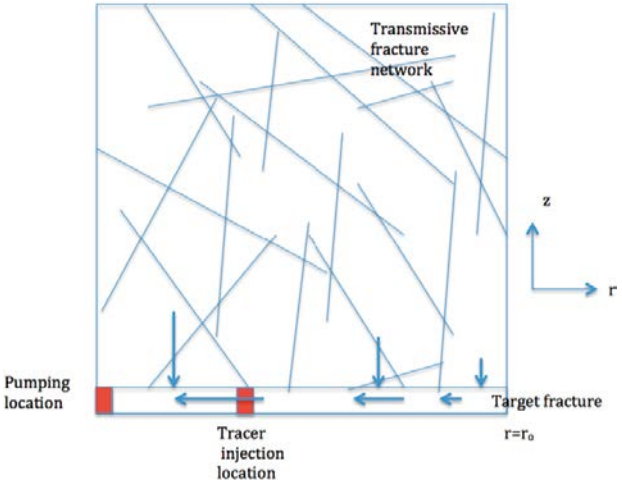

Figure A-2. *Illustration of fracture for a tracer test in a fractured rock with a network of conducting fractures. The small red rectangles indicate the packed off sections in the vertical pumping and injection boreholes, not shown.*

In the centre of the horizontal circular slot, there is a cylindrical hole with radius r_i and with height z_i. On the cylindrical sides of this hole the, the pumping section, the hydraulic head is h_i. At the outer radius r_o of the region and the flat top at z_o the head is h_∞. The other sides are closed to flow.

The boundary conditions then are

$$h(r = r_i,\ 0 < z < z_i) = h_i,$$
$$h(r = r_o,\ 0 < z < z_o) = h_\infty$$
$$h(r_i < r < r_o,\ z = z_o) = h_\infty \qquad \text{(A-5)}$$

r_i is the radius of the pumping borehole.

The solution is obtained by Wolfram Mathematica (Wolfram 2018) routine *NDSolve* based on finite elements in the form of an interpolation function for $h(r,z)$. It is used to calculate the inflow to the fracture at $r=r_o$ from

$$Q_{in} = Q(r_o, 0 < z < z_i) = -T\ 2\pi\ r_o \left.\frac{dh}{dr}\right|_{r=r_o} \qquad \text{(A-6)}$$

In the same way, the flow into the pumping section is

$$Q_{out} = Q(r_i, 0 < z < z_i) = -T\ 2\pi\ r_i \left.\frac{dh}{dr}\right|_{r=r_i} \qquad \text{(A-7)}$$

The difference is the flowrate that leaks in from the rock matrix.

It should be noted that in contrast to when the rock is tight and thus has a conductivity that is zero the fracture is constantly fed with water from the fractured rock and the flowrate is increased constantly approaching the pumping hole. This is in contrast to the non-leaking rock where the same flowrate goes into the fracture as out through the pumping hole.

When there is no leakage from the rock the hydraulic head is obtained from

$$h(r) = (h_\infty - h_i)\frac{\ln(\frac{r}{r_i})}{\ln(\frac{r_o}{r_i})} + h_i \qquad \text{(A-8)}$$

and the flowrate to the pumping section is

$$Q_{Noleak} = T\ 2\pi \frac{(h_\infty - h_i)}{\ln(\frac{r_o}{r_i})} \qquad \text{(A-9)}$$

When there is leakage the flowrate $Q(r)$ varies with r. In both cases the velocity in the fracture varies with radius as

$$u(r) = \frac{Q(r)}{\delta_m 2\pi r} = \frac{T}{\delta_m}\frac{dh(r)}{dr} \qquad \text{(A-10)}$$

δ_m denotes mass balance aperture of the fracture. In modelling the fracture as a porous medium with thickness z_i the porosity of this zone is

$$\varepsilon_{slot} = \frac{\delta_m}{z_i} \qquad \text{(A-11)}$$

The residence time for a tracer injected at $r = r_{inject}$ is

$$t_w = \int_{r_i}^{r_o} \frac{1}{u(r)} dr = \int_{r_i}^{r_o} \frac{\delta_m}{T\frac{dh(r)}{dr}} dr \qquad \text{(A-12)}$$

The ratio of residence time in the leaking fracture to the non-leaking is

$$t_{ratio} = \frac{\int_{r_i}^{r_o} \frac{1}{\left.\frac{dh(r)}{dr}\right|_{leak}} dr}{\int_{r_i}^{r_o} \frac{1}{\left.\frac{dh(r)}{dr}\right|_{Noleak}} dr} \qquad \text{(A-13)}$$

$\left.\frac{dh(r)}{dr}\right|_{leak}$ is evaluated as a mean over $0<z<z_i$.

The leaking flowrate, in addition to the difference between $Q_{out} - Q_{in}$ from Equations (A-6) and (A-7) can also be evaluated by integration of the leak flow along the flowpath.

$$Q_{leak} = -2\pi\ K_{rock} \int_{r_i}^{r_o} r \left.\frac{dh(r,z)}{dz}\right|_{z=z_{i+}} dr \qquad \text{(A-14)}$$

z_{i+} indicates that the gradient is evaluated on side of the rock at the interface between fracture and rock. Equation (A-14) is used to compare the results from Equations (A-6) and (A-7) .

It is to be noted that all flowrates and t_{ratio} do not depend on the aperture δ_m, which is not known. Only the absolute values of the residence times depend on δ_m.

A6 Experimental evidence of impact of leakage,

A6.1 The TRUE experiment

A number of tracer tests were performed in a fracture called Feature A in the Äspö Underground Rock Laboratory. These experiments are well documented and considerable effort has been spent to study the fractures, their hydraulic properties and sorption properties of the rock matrix and other minerals in the fractures (Winberg et al. 2000, Byegård et al. 2017). The experiments were made at a depth of about 400 m. In the analysis of the results, no leakage into the fracture from the rock was considered although it was seen from the hydraulic tests that flow dimensions were around 3 in the main fracture, Feature A, in which the tracer tests were made. Neretnieks (2002) and Neretnieks and Moreno (2003) analysed these experiments because the results suggested that Feature A should have a mean aperture of around 2.4 mm over its entire extent based on the flowrate and residence times according to Equation A-1). This was surprizing because the cubic law aperture was orders of magnitude smaller. Causes for the surprisingly large aperture were sought.

The possibility of leakage from the rock was explored by studying the hydraulic properties of the rock around Feature A. Five long boreholes ranging from 18 to 60 m had been drilled intersecting Feature A. Inflow measurements had been made every 0.5 m in these boreholes. These data were not reported as part of the TRUE experiments but are available in SKB's Sicada[1] data-base. These data were used by Neretnieks and Moreno (2003) to determine the average flowing fracture spacing, *S,* and the transmissivity distribution of the fractures.

A6.2 Analysis of the borehole flowrate data

162, 0.5 m sections were measured for flow. Of these 112 were found to carry water. In addition, a few sections varying in length between 1 and 8 m were found to carry water. The latter sections were not used in the analysis. About 30 % of the 0.5 m sections were carrying no or so low flowrates that these were below detection level. This number indicates that the average channel distance is slightly smaller than the section length 0.5 m (Moreno et al. 2001). The transmissivity distribution is shown as histogram in Figure A-3. It is reasonably well described by a ^{10}log-normal distribution with a mean of $\mu = -8.3$ and standard deviation $\sigma = 0.97$.

Based on the data in Winberg et al. (2000) the five locations intersecting Feature A have a mean $\mu = -7.7$ and standard deviation $\sigma = 0.62$. A statistical F-test shows that there is a probability of 40 % that Feature A variance is different from the rest of the population. A t-test shows that there is 80–90 % probability that their logarithmic means differ. It may be noted that the transmissivity in the five locations in Feature A varies between 0.85×10^{-8} and 3.9×10^{-8} m^2/s in four of the five locations but that in one location it is 32×10^{-8} m^2/s (Winberg et al. 2000). This is the section in which the pumping took place in the tracer experiment discussed. In the later over-coring of that section, resin injection showed five very closely lying fractures with a mean summed aperture of 0.45 mm, whereas in the injection location only one fracture was found with about ten times smaller aperture (Byegård et al. 2017). This will later be used as an argument that the pumping location may not be representative of Feature A and that it has a large impact on assessing the mass balance aperture. In the hydraulic tests, it was found that the flow dimension was 2.6 in the five locations in Feature A (Winberg et al. 2000). This suggests that hydraulically the flow may contain a non-negligible component of three-dimensional flow toward a local sink. This possibility was suggested by Neretnieks and Moreno (2003) and will be explored here also.

[1] SKB's data base on field and laboratory measurements. It can be accessed with permission from the SKB company: www.skb.se

For the subsequent modelling, the *arithmetic* mean T_a of the transmissivity is needed. This is obtained from

$$T_a = e^{\left(\mu_{Ln} + \frac{\sigma_{Ln}^2}{2}\right)} \qquad \text{(A-15)}$$

$\mu_{Ln} = \ln(10) \times \mu$ and $\sigma_{Ln} = \ln(10) \times \sigma$ where ln stands for natural logarithm. The mean of the transmissivity is $T_{aRock}=6.07\times10^{-8}$ m^2/s for the fractures in the rock and $T_{aA}=5.53\times10^{-8}$ m^2/s for Feature A respectively. It is at first surprising that Feature A is less transmissive. It is due to the smaller variance as can be understood from Equation (A-15). Using the values for the five points directly, instead of first determining μ and σ and then to use (6.1) to determine the mean transmissivity in Feature A, gives $T_{a,A}=7.9\times10^{-8}$ m^2/s. In all, this suggests that statistically there is no difference between the transmissivities of the background fractures and Feature A.

With the average distance S of about 0.5 m between the transmissive background fractures, the mean hydraulic conductivity of the rock matrix will be about $K = 3 \times T_a/S = 3 \times 6.07\times10^{-8}/0.5 = 3.64\times10^{-7}$ m/s. The factor 3 comes from the assumption that the fractures are randomly oriented in three dimensions.

For later use the following is noted for the fractures in the network: The arithmetic mean aperture from the cubic law is 0.0418 mm. The rock porosity is 0.000251.

The distance between injection and pumping section in the experiment considered here was $r_o=4.68$ m. Over an area of $\pi\, r_o^2$ a considerable number of fractures in the rock matrix will intersect Feature A. For the TRUE experiment this suggest that the leaking rock can be expected to impact the actual flowrate carried by water to be used in Equation (A-1).

A6.3 Modelling the TRUE experiments with a leaking fracture

The fractures in the TRUE site have a mean spacing of about 0.5 m, which suggests that a considerable number of them can intersect Feature A between the injection and the pumping locations. The transmissivities of the background fractures and that of Feature A are not very different as shown in Chapter 5. Two situations are explored below. In the first, it is assumed that Feature A can be described as a large flat fracture that extends continuously at least a radial distance of 5 m. The network of fractures in the surrounding rock is modelled to behave as a homsogeneous porous medium. Then the model described in Chapter 5 is used to describe the head and flowrate distributions. Three examples are presented. In the first case, example 1, there is no difference in transmissivities of Feature A and background fractures. In the second and third case, the transmissivity of feature A is two and four times larger than the background fractures respectively.

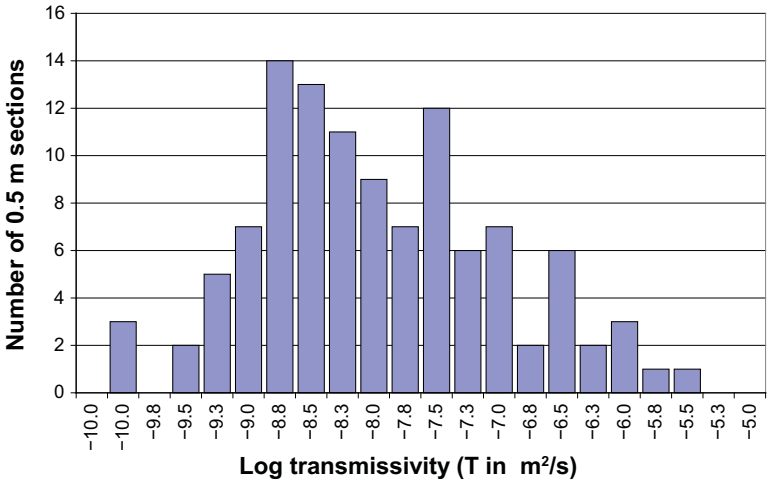

Figure A-3. *Frequency of transmissivities in five boreholes around Feature A.*

Then considering that, as in the first case, Feature A is no different than the other fractures, and that the entire medium is a three-dimensional network of fractures (or channels) it is modelled as if the flow-pattern is spherical to the pumping location.

A6.3.1 Example: Flowrates in leaking fracture

The distance between the pumping and injection locations is 4.68 m. The radius of pumping borehole is 0.028 m. Pumping takes place near r=0 and z=0 and a head difference of 10 meters is imposed between pumping hole and the outer boundaries r_o and z_o. This is about the actual head difference imposed in the experiment by pumping. The value of z_o is chosen to be the same as the distance between the injection and pumping location with the argument that because Feature A and the other fractures have similar transmissivities the draw-downs at similar distances will be similar. The aperture of Feature A is exaggerated in Figure A-4 for illustration purposes. The figure shows that the head drop mostly occurs near to the pumping location and that the water is also drawn into Feature A – the right-hand border in the picture- in the negative z-direction.

Table A-1. Predicted pumping rates, t_{ratio}´s and residence times, T_A/T_{BG} means ratio of transmissivities in feature and in background fractures.

Case	1	2	3	Comment
T_A/T_{BG}	1	2	4	δ_m NOT needed
t_{ratio}	14.0	8.04	4.80	δ_m NOT needed
Q_{leak} l/hr	2.71	4.79	8.27	δ_m NOT needed
Q_{Noleak} l/hr	1.34	2.68	5.36	δ_m NOT needed
t_{leak} hr	15.2	4.64	1.30	cubic law used

Q_{leak} is the predicted flowrate when the fracture is also supplied with water from the leaking rock. Q_{Noleak} is the flowrate when all water comes only through Feature A. The results for the t_{ratio} in Table A-1 depend only on the transmissivities and not on the absolute value of the flowrates. It is seen that the flowrate, when there is leaking, would in case 1 be 2 times larger than if there is no leaking. If the lower t_w is used in Equation (A-1) for the experimentally measured flowrate the predicted mass balance aperture would be 0.15 mm instead of 2.4 mm, which is more reasonable.

The flowrate (pumping rate) in this TRUE experiment was 24 l/hr. The flowrate was obviously not well predicted in this modelling.

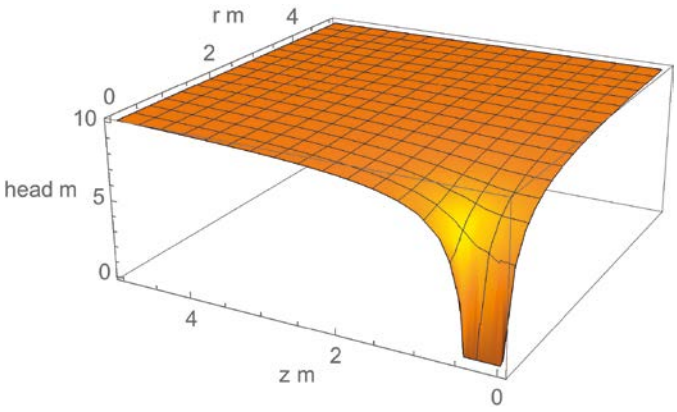

Figure A-4. *Head distribution in Case 1.*

A6.3.2 Example: Fracture apertures and water residence time

The residence time of the tracer in the experiments was about 8 hours, from which information on the non-leaking fracture aperture should be 2.4 mm according to Equation (A-1). This is an impossibly large mean fracture aperture for an individual fracture. It could, however, be a possible value for a fracture zone with crushed rock fragments and many small particles that give rise to high porosity, much friction and leads to the low transmissivity. Neretnieks (2002) showed that when a fracture zone actually itself can be seen as a porous medium consisting of many small particles, that are themselves porous, both porosities can contribute to the water volume available to the tracer to reside in and lead to longer tracer residence time without affecting the flow residence time of the water. It may also potentially add considerably to the amount of surface available to sorbing tracers and their retardation. It was also shown that when there is channelling the presence of stagnant waters adjacent to the channels can considerably contribute to the water volume available to the tracers.

If the transmissivity of Feature A is governed by the friction in one smooth parallel walled slot the aperture can be determined by the cubic law, Equation (A-2) and is δ_c = 0.046 mm for $T_{a,A}$=7.9×10^{-8} m^2/s. This is more than 50 times smaller than δ_m = 2.4 mm obtained from Equation (A-1). This is in line with the differences presented in Chapter 3 for other tracer experiments, but it gives no information on why the flowrate is so poorly predicted. As shown in Table A-1 an increase in the transmissivity of Feature A increases the predicted flowrate but not enough to come close to the measured value.

A6.4 Spherical flow pattern

A6.4.1 Example: Spherical flow flowrate

In the densely fractured rock, Feature A might be considered not to have special status but be just one of the stochastic fractures. In that case, it may be more appropriate to model the flow pattern around a sink- the pumping location- as being spherical rather than cylindrically radial in Feature A with a leaking rock matrix. Assuming that the cubic law aperture, δ_c = 0.046 mm, is a fair approximation of the mass balance aperture, the flow porosity of the rock with the mean spacing S=0.5 m is $\varepsilon_{rock} = \frac{3\delta_c}{S} = 0.00028$.

Spherical flowrate can be calculated by

$$Q_{sph} = K_{rock}\,\pi\,\frac{(h_\infty - h_i)}{\frac{1}{r_i} - \frac{1}{r_o}} \qquad \text{(A-16)}$$

The residence time is obtained from the flow volume of the sphere divided by the flowrate

$$t_w = \frac{\frac{4}{3}\pi(r_o^3 - r_i^3)\varepsilon_{rock}}{Q_{sph}} \qquad \text{(A-17)}$$

The flowrate and residence time predicted with Equations (A-16) (A-17) is 1.2 l/hr and 94 hours respectively for the case when Feature A is not different from the background fractures. Inspecting Equation (A-16) shows that the flowrate is in practice directly proportional to r_i because r_o is so very much larger than r_i.

The pumping location has a transmissivity that is more than an order of magnitude larger than the mean of the other four locations intersecting Feature A. This together with the large aperture measured by resin injection, 0.45 mm, suggests that the flowrate to the pumping location is more determined by the lower transmissivity at locations further from the pumping location. For the modelling with Equation (A-16) this means that the pressure drop, which is essentially set by the flow nearest radius r_i considerably overestimates the pressure drop. A larger value of r_i could be used to compensate for this. Table A-2 shows the predicted flowrate and water residence time when r_i is increased to 0.5 m. Then essentially the experimental results are obtained.

Table A-2. Impact of radius of pumping location r_i.

Example	Cylindrical	Spherical	Experiment
Pumping radius r_i m	0.5	0.5	0.028
Q, l/hr	Q_{leak} = 8.85	Q_{sph}= 22.9	Q_{exp}= 24
t, hr	t_{leak} = 4.07	t_{sph} = 5.73	t_{sph} = 8

This comes much closer to the experimentally found values both for the flowrate and the residence time, for the leaking fracture as well as for the spherical flow case.

The spherical flow case has also been used earlier to predict the breakthrough curves for sorbing tracers. Neretnieks and Moreno (2003), by assuming that feature A stochastically was not different from the background rock matrix predicted the breakthrough curves for the three sorbing tracers Cs, Rb, and Ba used in the TRUE experiment. For strongly sorbing tracers the *water* residence time is negligible compared to the residence time of the tracer that is retarded by sorption on the fracture surface and in the rock matrix and therefore in practice not influenced by fracture aperture. The residence time is dominated by the magnitude of the fracture surface, the so-called flow wetted surface, FWS, that the flowrate Q contacts underway. The predicted results were surprisingly good considering that the predictions used only the FWS, the pumping rate and the sorption and matrix diffusion coefficients; all of which were obtained independently and no adjustments of any parameters were made.

A7 Discussion and conclusions

As shown in Chapter 3, the apertures derived from pumping tracer test are several, up to many, orders of magnitude larger than what visible inspections find. The choice of a fracture for a tracer test will naturally be one in which a high flowrate channel is intersected. A fracture is seldom so isolated that it is only fed by other fractures at its perimeters. It is possible and even likely that a fracture is intersected by many other fractures in the network between tracer injection location and pumping location. This was demonstrated in the so-called TRUE experiment where the surrounding rock also had been investigated, that such leakage could feed the target fracture with a much larger flowrate than what is fed by the target fracture itself. This leads to considerable overestimation of water residence time in the target fracture and thus of its aperture.

The mass balance apertures in individual fractures in Figure A-1 are surprisingly large considering that they are mean values for fractures that extend over often tens of meters or more. Most fractures with transmissivities less than 10^{-6} m^2/s in Figure A-1 are individual fractures. So large apertures over any extent are not visually observed in drifts and tunnels in Äspö and Stripa, from which most of the data are taken. Recent follow-up investigations of Feature A have shown that the studied fractures of Feature A show an accumulated average physical aperture of 0.45 mm, with a variation in aperture in the span 0–1 mm (Byegård et al. 2017). This is much less than the mass balance aperture of around 2.4 mm derived by Equation (A-1).

No definite, single, clear-cut reason has been found for the large discrepancy between mass balance aperture evaluated from pumping tracer tests and cubic law and physically observed apertures. However, the combination of channelling, leaking rock matrix and diffusion into stagnant water zones is deemed to very likely exaggerate the aperture by one to two orders of magnitude.

The mass transport to and from water in fractures that intersect a buffer or backfill in nuclear waste repositories will largely be proportional to the aperture that defines the mobile volume i.e. the mass balance aperture. However, the mass balance aperture as evaluated from tracer tests overestimates this entity by about two orders of magnitude for individual fractures. The cubic law aperture, possibly with a slight correction, better represents the physical or mass balance aperture.

For fracture zones with crushed rock, the physical width can usually be seen in cores from boreholes. The porosity can usually be at least approximately assessed from this information also.

Arkitektkopia AB, Bromma, 2019

SKB is responsible for managing spent nuclear fuel and radioactive waste produced by the Swedish nuclear power plants such that man and the environment are protected in the near and distant future.

skb.se